Electronic Supplementary Material (ESI) for Nanoscale.

Supporting Information

Accurate Electronic Properties and Nonlinear Optical Response of Two-dimensional MA_2Z_4

Jia-Shu YANG[1], Luneng Zhao[1], Shi-Qi LI[1]*, Hongsheng Liu[1], Lu Wang[2], Maodu Chen[1], Junfeng Gao[1]*, Jijun Zhao[1]

1. Key Laboratory of Materials Modification by Laser, Ion and Electron Beams, Dalian University of Technology, Ministry of Education, Dalian 116024, China

2. Institute of Functional Nano & Soft Materials (FUNSOM), Jiangsu Key Laboratory for Carbon-Based Functional Materials & Devices, Soochow University, Suzhou, Jiangsu 215123, China

S1 The second-order coefficients for MA_2Z_4 family

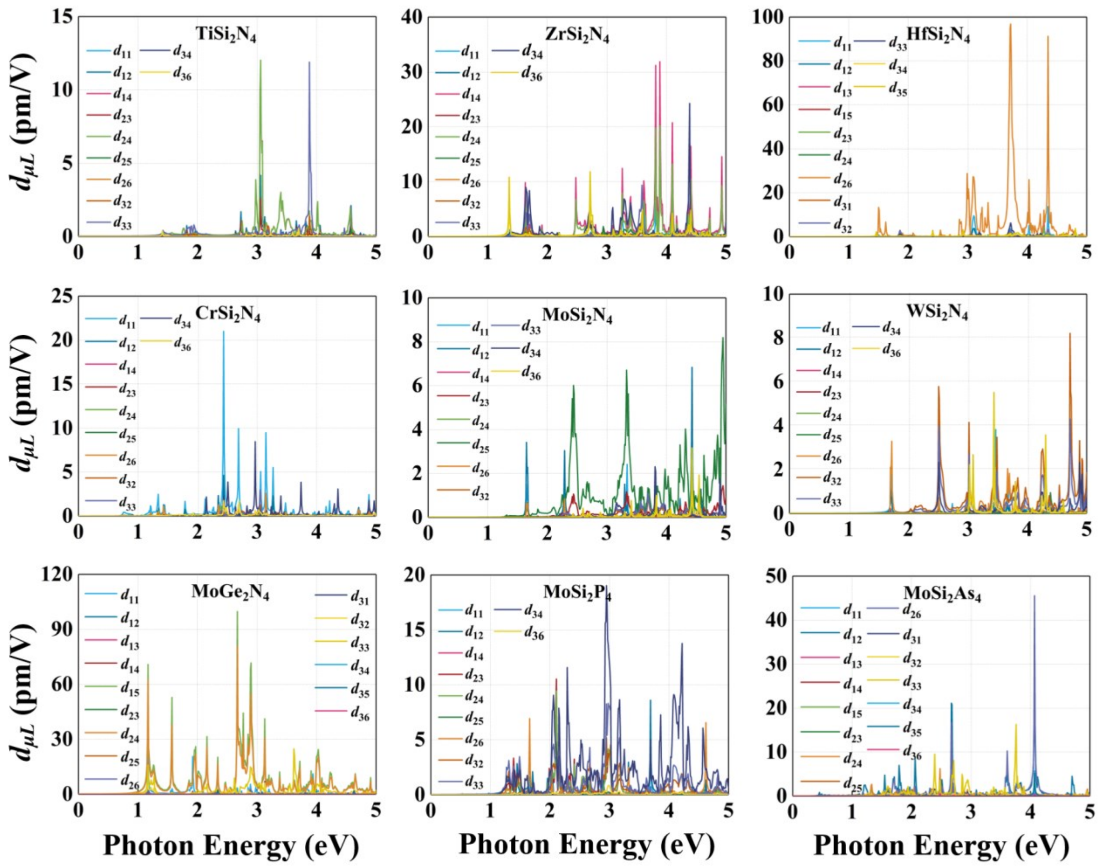

Figure S1. Besides the large d_{16}, d_{21} and d_{22}, other small nonlinear coefficients of second-order susceptibilities of explored MA_2Z_4.

S2 Photon energy-dependent imaginary and real components of second-order coefficients for MA_2Z_4 family

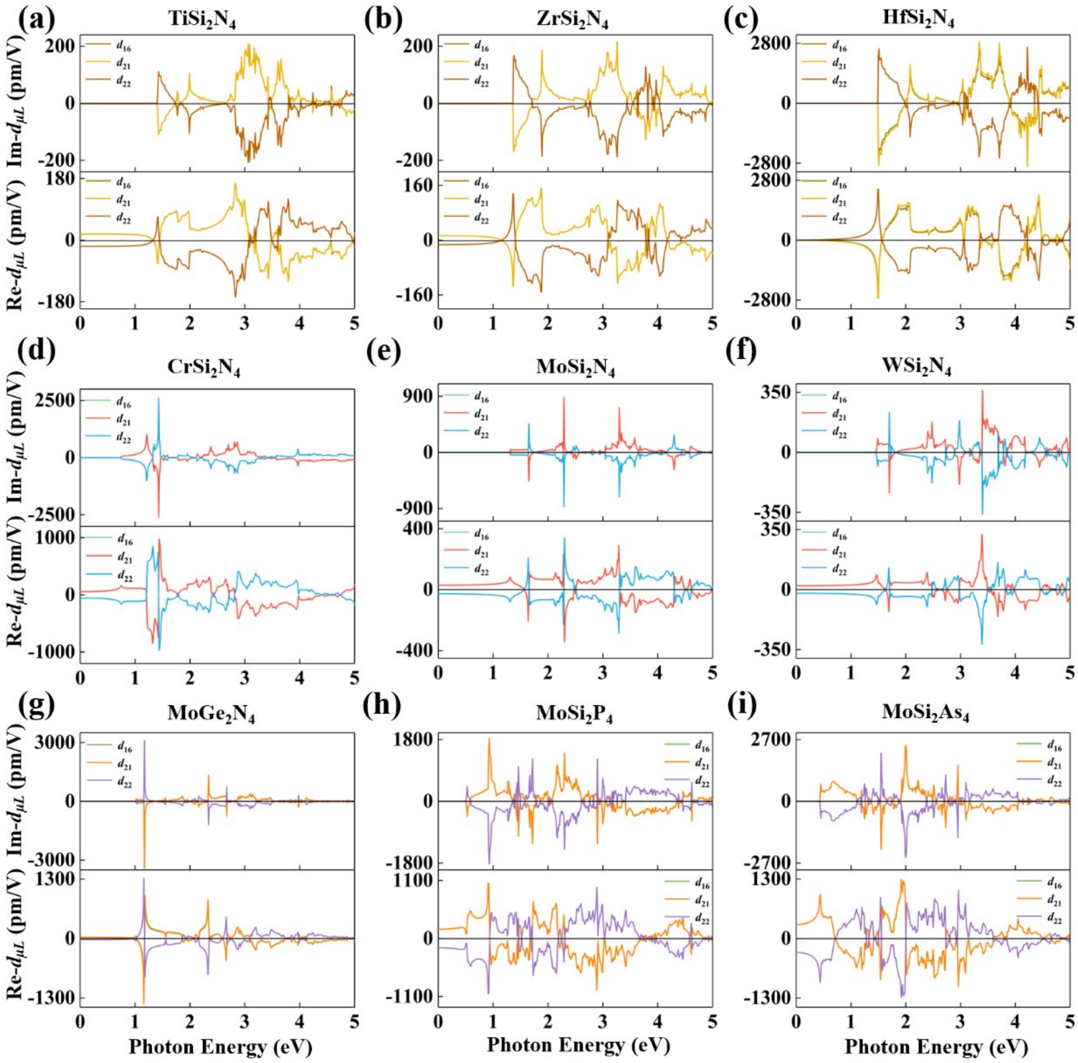

Figure S2. Photon energy-dependent imaginary and real components of second-order coefficients for MA_2Z_4 family.

S3 Polar plot of SHG intensity as a function of azimuthal angle and incident angle

Considering the sample shed by the linearly polarized pump light with an incident angle θ, the electric field of the pump light can be given as follows:

$$\begin{bmatrix} E_x \\ E_y \\ E_z \end{bmatrix} = \begin{bmatrix} E_0 \cos[\theta] \\ 0 \\ E_0 \sin[\theta] \end{bmatrix}$$ * MERGEFORMAT (S1)

The relationship between the second order nonlinear susceptibility $\chi_{ijk}^{(2)}$ and the second-order nonlinear coefficient $d_{\mu L}$ can be described as:

$$d_{\mu L} = \frac{1}{2}\chi_{ijk}{}^{(2)} = \begin{bmatrix} d_{11} & d_{12} & d_{13} & d_{14} & d_{15} & d_{16} \\ d_{21} & d_{22} & d_{23} & d_{24} & d_{25} & d_{26} \\ d_{31} & d_{32} & d_{33} & d_{34} & d_{35} & d_{36} \end{bmatrix}$$ * MERGEFORMAT (S2)

By the use of rotation operation $T(\phi)$, we can obtain the transformed tensor containing azimuthal angle:

$$d_{i,j,k}^{(2)}{}' = \sum_{f=1}^{3} T_{i,f} \times \sum_{g=1}^{3} T_{j,g} \times \sum_{h=1}^{3} T_{k,h} \times d_{f,g,h}^{(2)}$$ * MERGEFORMAT (S3)

$$T(\phi) = \begin{bmatrix} \cos[\phi] & \sin[\phi] & 0 \\ -\sin[\phi] & \cos[\phi] & 0 \\ 0 & 0 & 1 \end{bmatrix}$$ * MERGEFORMAT (S4)

Here ϕ is the azimuthal angle between the mirror plane in the crystal structure and the polarization of the pump beam. $T_{i,f}, T_{j,g}, T_{k,h}$ is a component in $T(\phi)$. Thus the SHG elements can be expressed as:

$$\begin{bmatrix} P_x(2\omega) \\ P_y(2\omega) \\ P_z(2\omega) \end{bmatrix} = 2\varepsilon_0 d'_{\mu L}(\phi) \begin{bmatrix} E_x^2(\omega,\theta) \\ E_y^2(\omega,\theta) \\ E_z^2(\omega,\theta) \\ 2E_y(\omega,\theta)E_z(\omega,\theta) \\ 2E_z(\omega,\theta)E_x(\omega,\theta) \\ 2E_x(\omega,\theta)E_y(\omega,\theta) \end{bmatrix}$$ * MERGEFORMAT

(S5)

where ε_0 represents the permittivity of the space.

With the calculated nonzero second-order nonlinear coefficients and their relationship, the SHG polarization components from MA_2Z_4 can be expressed as:

$$P_{MA_2Z_4} = \begin{bmatrix} P_x \\ P_y \\ P_z \end{bmatrix} = 2\varepsilon_0 \begin{bmatrix} -d_{22}E_0^2 \cos^2[\theta]\sin[3\phi] \\ -d_{22}E_0^2 \cos^2[\theta]\cos[3\phi] \\ 0 \end{bmatrix}$$ *

MERGEFORMAT (S6)

Thus, the two polarization components (parallel and perpendicular) of SHG intensity as a function of azimuthal and incident angle can be described as:

$$I_{//} \propto \left[-P_x\left(d_{\mu L},\phi\right)\cos[\theta] + P_z\left(d_{\mu L},\phi\right)\sin[\theta]\right]^2$$ *

MERGEFORMAT (S7)

$$I_{\perp} \propto P_y^2\left(d_{\mu L},\phi\right)$$ * MERGEFORMAT (S8)

Lastly, the $I_{//}$ and $I_{\perp}$ from MA_2Z_4 can be expressed as:

$$I_{//} \propto d_{22}^2 \sin^2[3\phi]\cos^4[\theta]$$ * MERGEFORMAT (S9)

$$I_{\perp} \propto d_{22}^2 \cos^2[3\phi]\cos^4[\theta]$$ * MERGEFORMAT (S10)

S4 Polar plots of SHG intensity from MA_2Z_4 family under different incident photon energy

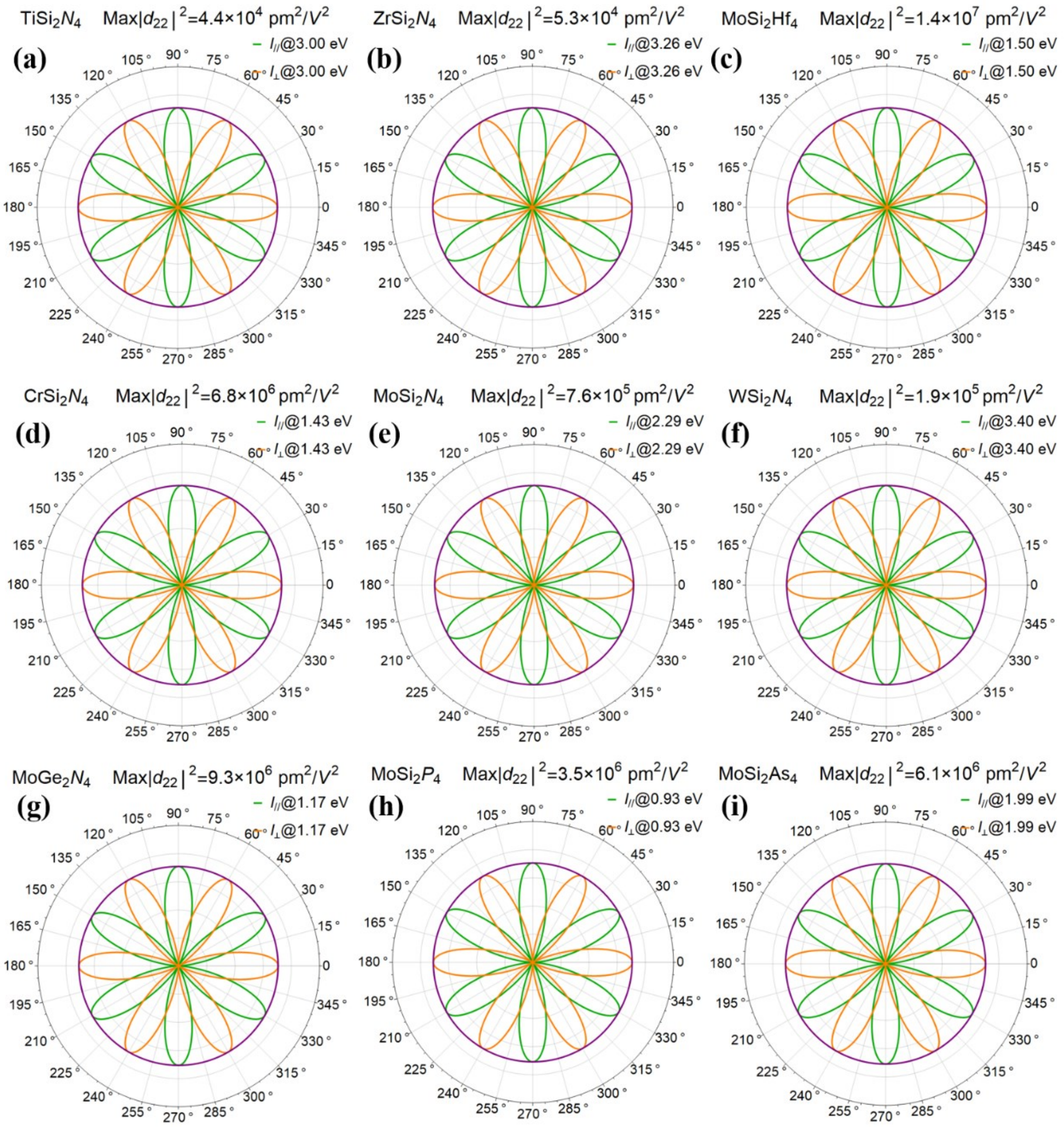

Figure S4. Polar plots of the SHG intensity from MA_2Z_4 as a function of the crystal's azimuthal angle under different photon energy. Their maximum values are represented by the purple circles in the polar plot and listed on the top.

S5 All the locations of prominent peaks and their corresponding d_{22} in MA_2Z_4 family

Compound	d_{22} (pm/V) @ E_1	d_{22} (pm/V) @ E_2	d_{22} (pm/V) @ E_3	d_{22} (pm/V) @ E_4	d_{22} (pm/V) @ E_5	d_{22} (pm/V) @ E_6	d_{22} (pm/V) @ E_7
$TiSi_2N_4$	116.26 @ 1.43 eV	120.73@ 1.99 eV	179.10 @ 2.84 eV	210.75 @ 3.00 eV	209.40 @ 3.06 eV	195.28 @ 3.17 eV	161.10 @ 3.66 eV
$ZrSi_2N_4$	201.71 @ 1.37 eV	207.92 @ 1.89 eV	147.19 @ 2.95 eV	183.18 @ 3.08 eV	229.84 @ 3.26 eV	128.26 @ 3.78 eV	137.93 @ 4.10 eV
$HfSi_2N_4$	3697.04 @ 1.50 eV	1632.08 @ 1.85 eV	1929.53 @ 2.08 eV	2575.91 @ 3.34 eV	2665.56 @ 3.71 eV	2619.93 @ 4.22 eV	2115.52 @ 4.44 eV
$CrSi_2N_4$	1012.17 @ 1.21 eV	900.43 @ 1.33 eV	2608.85 @ 1.43 eV	582.02 @ 2.70 eV	747.84 @ 2.86 eV	414.39 @ 3.19 eV	382.10 @ 3.97 eV
$MoSi_2N_4$	471.62 @ 1.65 eV	870.82 @ 2.29 eV	737.41 @ 3.30 eV	256.51 @ 3.58 eV	281.23 @ 4.30 eV		
WSi_2N_4	239.61 @ 1.70 eV	147.50 @ 2.40 eV	176.72 @ 2.48 eV	184.53 @ 2.98 eV	441.19 @ 3.40 eV	199.41 @ 3.68 eV	129.83 @ 4.17 eV
$MoGe_2N_4$	3042.65 @ 1.17 eV	1294.50 @ 2.34 eV	764.71 @ 2.67 eV				
$MoSi_2P_4$	1874.79 @ 0.93 eV	1085.45 @ 1.46 eV	1295.03 @ 1.72 eV	1129.80 @ 2.16 eV	1403.39 @ 2.30 eV	1345.30 @ 2.90 eV	
$MoSi_2As_4$	1052.39 @ 0.45 eV	2143.43 @ 1.55 eV	2464.77 @ 1.99 eV	1017.45 @ 2.23 eV	1163.34 @ 2.73 eV	1674.23 @ 2.95 eV	969.74 @ 3.10 eV

Table S1. All the locations of prominent peaks and their corresponding d_{22} in MA_2Z_4 family.